New Experiments Towards Understanding the Enduring Puzzle of the Exchange Bias Effect

Paul Hyde[1], Neele Grenda[2], Ko-Wei Lin[3], Yongsheng Gui[1], Johan van Lierop[1], Byron Southern[1], Can-Ming Hu[1]
[1]Department of Physics and Astronomy, University of Manitoba
[2]University of Hamburg, Germany
[3]National Chung Hsing University, Taiwan

Abstract

We conducted in-plane ferromagnetic resonance (FMR) measurements on a Permalloy ($Ni_{80}Fe_{20}$) layer coupled to an antiferromagnetic NiO layer. These measurements, performed at medium to weak external field strengths, allow us to map the FMR frequency as a function of the applied field. The relation of these parameters has never before been measured for low external field strengths, and the obtained dispersion curves show features significantly deviating from the predictions of current FM/AFM interface models. A new model taking into account rotational anisotropy in the AFM has been developed which explains the observed characteristics, yielding new insights into the governing interactions at the FM/AFM interface.

Motivation

When ferromagnetic (FM) and antiferromagnetic (AFM) materials are held next to each other, we would intuitively expect the behaviour of the FM moments to be unaffected by the normally non-magnetisable AFM. However, experiments performed over the past 50 years have indicated otherwise; revealing several unusual effects seen only in these FM/AFM systems. The most prominent of these effects, known as exchange bias, results in the FM material feeling a net force from the AFM material in one particular direction. Although this effect has found significant commercial use as a simple way to maintain the magnetization of reading and recording heads in data storage technologies, its atomic basis has remained unknown. The overall lack of experimental techniques capable of probing the behaviour of the magnetic moments near the FM/AFM interface has resulted in most of the theories attempting to explain the origins of exchange bias being merely theoretical and based on limited experimental evidence. Thus, a new experiment providing original data concerning the behaviour of the interfacial magnetic moments in an FM/AFM system could provide information allowing us to better understand and perhaps produce new theories regarding the behaviour of these moments.

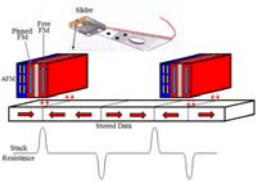

Figure 1: A schematic of how exchange bias is used in hard disk reading heads to hold the magnetization of a central FM layer

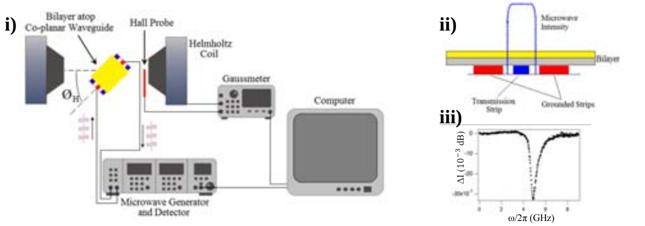

Figure 2: i) Schematic of the apparatus used to measure the FMR frequency within our FM/AFM bilayer. As our bilayer sample sits atop a co-planar waveguide (CPW), the Gaussmeter, using a Hall Probe to measure the external field on the sample, records and adjusts the strength of this field by controlling the current passing through a pair of Helmholtz coils. As this is being done, the microwave generator sends microwaves of different frequencies through the CPW and detects the transmitted microwave intensities at each frequency. **ii)** The intensity of the microwaves penetrating the sample decreases abruptly outside a small area above the transmission strip (2mm wide). **iii)** A plot of the difference between the microwave frequency intensities incident on our sample and those transmitted through it in an external field of 300G. The frequency at the minimum of the dip in this plot is the FMR frequency of our sample in a 300G external field.

Ferromagnetic Resonance

Much like a spinning top precesses about the direction of the earth's gravitational field, so too will an FM magnetic moment in the presence of a magnetic field precess about the vector direction of the field. The precession frequency, known as the ferromagnetic resonance (FMR) frequency, of these moments depends on the strength of the total magnetic field acting on them; in strong fields their radius of precession is small and (by conservation of angular momentum) their FMR frequency will be high, in weaker fields the precession radius of the moments is larger and their FMR frequency will be lower. If the frequency of a beam of radiation (such as microwave radiation) matches the FMR frequency of an FM material, it will be absorbed by the precessing moments, allowing the FMR frequency of a material to be determined by observing which frequency of radiation is most absorbed by its magnetic moments.

Measured Dispersion Curves

When measuring the angular dependence of the dispersion curves of our bilayer sample, we performed two separate sweep measurements. The Up Sweeps began in strong negative external fields and took measurements in gradually increasing field steps. The Down Sweeps began in strong positive fields and took measurements in gradually decreasing fields steps. These Up and Down Sweeps were observed to be distinct but symmetric with each other about approximately 0G, similar to plots of hysteresis curves. Working under the assumption that the difference between Up and Down Sweeps is due to a 180° transition in the magnetic structure of our bilayer system between strong positive and negative fields, we determined the field strength this transition occurs at by halting and reversing Up Sweeps and seeing whether the Reversed Sweep has Up Sweep characteristics (sweep has not crossed transition field) or Down Sweep characteristics (sweep has crossed transition field). Using this method the external field strength where the magnetic structure of our system undergoes a 180° transition was determined to be ~40G.

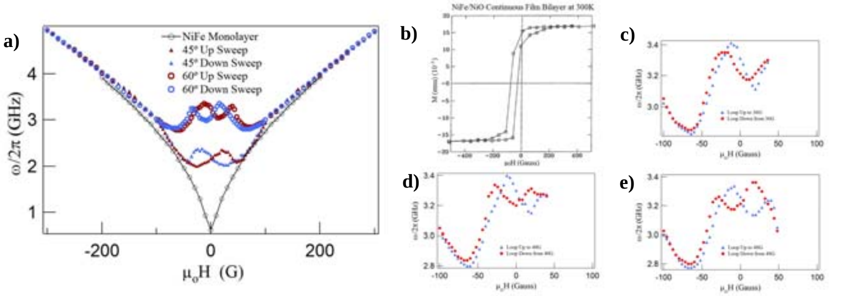

Figure 3: a) Experimentally measured Up and Down Sweep dispersion curves in our NiFe/NiO bilayer for external field angles ($Ø_H$) of 45° and 60° compared to the measured dispersion curve in an NiFe monolayer. All curves for $Ø_H$ values ≤45° were roughly equal to those for $Ø_H = 45°$ and all curves for $Ø_H$ values ≥60° were roughly equal to those for $Ø_H = 60°$. **b)** The measured easy-axis hysteresis curve of our bilayer, measured after being annealed in an external field. (note that our sample was only annealed after the measurement of our dispersion curves). The curve is not centred on zero external field due to the effects of exchange bias **c)-e)** $Ø_H = 90°$ Up Sweep loops stopped and reversed at 36G, 40G, and 48G. The Reversed Sweep from 36G has the characteristics of an Up Sweep, and the Reversed Sweep from 48G has the characteristics of a Down Sweep, while the Reversed Sweep from 40G has some features of both Up and Down Sweeps.

Cubic Anisotropy Theory

To explain the behaviour of the measured dispersion curves for our bilayer sample a new theory, called the Cubic Anisotropy Theory, was developed. The key concepts of this theory are:

- The AFM material is treated only as a source of anisotropy fields for the FM moments, no assumptions are made as to how this anisotropy arises
- 3 anisotropy directions, in the $\hat{x}$ and $\hat{x} \pm \hat{y}$ directions, are felt by the FM moments
- The exchange anisotropy field acts along the direction of the external field; in strong fields it acts parallel to the external field, and during measurement sweeps its direction flips 180° at 40G during Up Sweeps and at -40G during Down Sweeps.

The Energy stored within the FM moments in this theory is given by:

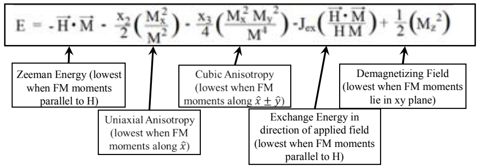

$$E = -\vec{H}\cdot\vec{M} - \frac{x_2}{2}\left(\frac{M_x^2}{M^2}\right) - \frac{x_3}{4}\left(\frac{M_x^2 M_y^2}{M^4}\right) - J_{ex}\left(\frac{\vec{H}\cdot\vec{M}}{HM}\right) + \frac{1}{2}\left(M_z^2\right)$$

Zeeman Energy (lowest when FM moments parallel to H)

Uniaxial Anisotropy (lowest when FM moments along $\hat{x}$)

Cubic Anisotropy (lowest when FM moments along $\hat{x} \pm \hat{y}$)

Exchange Energy in direction of applied field (lowest when FM moments parallel to H)

Demagnetizing Field (lowest when FM moments lie in xy plane)

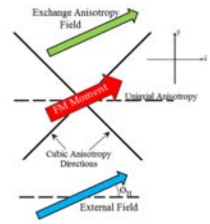

Figure 4: The various anisotropy directions felt by the FM moments according to the Cubic Anisotropy Theory

Where x_2, x_3, and J_{ex} are constants representing the strength of each anisotropy direction.

After converting to spherical coordinates, the azimuthal angle (Ø) and polar angle (θ) at each external field strength where the moment energy is minimized can be found by calculating:

$$\frac{\partial E}{\partial Ø} = 0 \qquad \frac{\partial E}{\partial \theta} = 0$$

With these angles calculated, the FMR frequency predicted by the Cubic Anisotropy Theory for each external field strength can be calculated using:

$$\left(\frac{\omega}{\gamma}\right)^2 = \frac{1}{M^2\sin^2\theta}\left(\frac{\partial^2 E}{\partial^2\theta}\frac{\partial^2 E}{\partial^2 Ø} - \left(\frac{\partial^2 E}{\partial\theta\partial Ø}\right)^2\right)$$

Predicted Dispersion Curves

The dispersion curves predicted by the Cubic Anisotropy Theory (Figure 5a) and c)) have a shape similar to the curves we obtained experimentally (Figure 5b) and d)); namely, for $Ø_H$ near 0° the curve has only one peak occurring in positive fields for Up Sweeps and negative fields for Down Sweeps, and for $Ø_H$ near 90° the curve has two peaks separated by a minima, which again occurs in positive fields for Up Sweeps and negative fields for Down Sweeps. The 180° flipping of J_{ex} at 40G for Up Sweeps (-40G for Down Sweeps) has the effect of reducing the depth of one of the outer minima in curves for $Ø_H$ near 0° and reducing the size of one of the maxima for curves near 90°, as is seen in the experimental curves. Remaining difficulties for the Cubic Anisotropy Theory include the fact that it predicts that the curves will evolve as $Ø_H$ changes (unlike our experimental curves which have the same shape provided $Ø_H$ remains either ≤45° or ≥60°) and that the FMR frequencies of the predicted curves are approximately 1-1.5GHz lower than those seen experimentally.

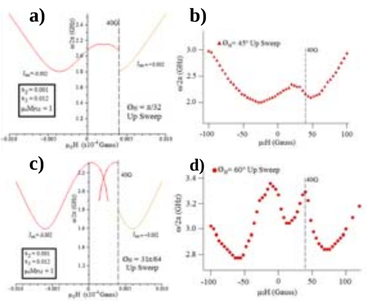

Figure 5: The Up Sweep dispersion curves predicted by the Cubic Anisotropy Theory for external field angles of **a)** π/32 and **c)** 31π/64 compared to the experimentally measured curves for external field angles of **b)** 45° and **d)** 60°. Predicted Down Sweep curves are simply the mirror images of Up Sweep curves.

Conclusions

The dispersion curves of an in NiFe/NiO bilayer were measured and were found to have characteristics not predicted by current theories which model the interaction between FM and AFM materials. Based on these characteristics, the Cubic Anisotropy Theory was developed. This theory can explain the observed characteristics of the measured dispersion curves, but is unable to perfectly reproduce the measured dispersion curves for all angles $Ø_H$. Possible solutions to the Cubic Anisotropy Theory's difficulties, such as allowing the entire magnetic structure produced by the AFM to rotate either parallel or anti-parallel to the external field or letting each FM moment rotate independently, are currently being incorporated into the theory with promising results. The new data and theory examined here contain fresh information about the poorly understood interactions between FM and AFM materials; information which could help us to understand and improve the mechanisms used in magnetic data storage technology.

Acknowledgements

Thank you to the other members of the Dynamic Spintronics Group for their support, and to the Nanomagnetism Research Group for performing the hysteresis measurements on our sample.

[1] W. H. Meiklejohn, C. P. Bean, *New Magnetic Anisotropy*, Phys. Rev. **105**, 904 (1957)

[2] J. Smitt, H.G. Belgers, Phillips Res. Rep. 10, 113 (1955)

[3] K.-W. Lin, M. Mirza, C. Shueh, H.-R. Huang, H.-F. Hsu, J. van Lierop, Appl. Phys. Lett. (2012)